Akt/mTOR pathway is a crucial regulator of skeletal muscle hypertrophy and can prevent muscle atrophy *in vivo*

Sue C. Bodine*‡, Trevor N. Stitt*, Michael Gonzalez*, William O. Kline*, Gretchen L. Stover*, Roy Bauerlein*, Elizabeth Zlotchenko*, Angus Scrimgeour†, John C. Lawrence†, David J. Glass* and George D. Yancopoulos*‡

*Regeneron Pharmaceuticals, Inc. 777 Old Saw Mill River Road, Tarrytown, New York 10591-6707, USA

† Departments of Pharmacology and Medicine, University of Virginia, Charlottesville, Virginia, 22908, USA

‡e-mail: sue.bodine@regeneron.com or george@regeneron.com

Skeletal muscles adapt to changes in their workload by regulating fibre size by unknown mechanisms[1,2]. The roles of two signalling pathways implicated in muscle hypertrophy on the basis of findings *in vitro*[3–6], Akt/mTOR (mammalian target of rapamycin) and calcineurin/NFAT (nuclear factor of activated T cells), were investigated in several models of skeletal muscle hypertrophy and atrophy *in vivo*. The Akt/mTOR pathway was upregulated during hypertrophy and downregulated during muscle atrophy. Furthermore, rapamycin, a selective blocker of mTOR[7], blocked hypertrophy in all models tested, without causing atrophy in control muscles. In contrast, the calcineurin pathway was not activated during hypertrophy *in vivo*, and inhibitors of calcineurin, cyclosporin A and FK506 did not blunt hypertrophy. Finally, genetic activation of the Akt/mTOR pathway was sufficient to cause hypertrophy and prevent atrophy *in vivo*, whereas genetic blockade of this pathway blocked hypertrophy *in vivo*. We conclude that the activation of the Akt/mTOR pathway and its downstream targets, p70^{S6K} and PHAS-1/4E-BP1, is requisitely involved in regulating skeletal muscle fibre size, and that activation of the Akt/mTOR pathway can oppose muscle atrophy induced by disuse.

Initial studies in cardiac hypertrophy[3], as well as early studies with skeletal muscle cells *in vitro*[4,5], pointed towards a key role for the cyclosporin-inhibitable phosphatase known as calcineurin. We first examined the role of the calcineurin pathway in a model of compensatory muscle hypertrophy. When a fast-twitch skeletal muscle is subjected to a chronic workload increase by removing functionally synergistic muscles, the muscle compensates by increasing fibre size and muscle weight, as well as by switching fibres to a slow-twitch phenotype[8,9]. The switch to a slow fibre phenotype has recently been suggested to be under the control of a calcineurin-dependent pathway[10], although the Ras/MAPK (mitogen-activated protein kinase) pathway has also been implicated[11]. Functional overload of the rat plantaris muscle was induced by surgically removing the soleus and gastrocnemius muscles. Cyclosporin A (CsA) was given at a dosage (15 mg kg^{-1}, subcutaneously) sufficient to block completely the cardiac hypertrophy induced pharmacologically by the β_2-adrenergic agonist clenbuterol (Fig. 1a) and which inhibited calcineurin activity in control skeletal muscle (Fig. 1b, first two columns). Treatment with CsA was unable to prevent compensatory hypertrophy of the plantaris at 7, 14 or 30 days after the surgical overload, as shown by the increases in muscle weight (Fig. 1d) and fibre size (Fig. 1c, e). Furthermore, treatment with CsA had no effect on the percentage of fibres expressing slow myosin heavy chain (MyHC) after compensatory hypertrophy (Fig. 1c, f) or the shifts in MyHC expression (data not shown). Consistent with the lack of a role for calcineurin induction during compensatory hypertrophy, calcineurin activity was not increased but rather decreased in hypertrophying muscle (Fig. 1b, third column). Finally, treatment with FK506, a calcineurin inhibitor that functions through the binding of FK506-binding protein 12 (FKBP12), was unable to prevent the increase in muscle weight associated with compensatory hypertrophy (Fig. 1g).

We have found[6] that hypertrophy of myotubes induced *in vitro* by insulin-like growth factor 1 (IGF-1) depended on a pathway initiated by PtdIns-3-OH kinase (PI(3)K) and the PtdIns-regulated kinase Akt, which in turn led to activation of the rapamycin-sensitive kinase known as mTOR, whose downstream targets, p70^{S6K} and PHAS-1/4E-BP1, have been shown to promote protein synthesis through increases in translation initiation and elongation[12–16]. To obtain initial evidence for a role of the Akt pathway during muscle hypertrophy *in vivo*, we examined Akt phosphorylation in the model of compensatory hypertrophy of the plantaris described above. The amount of Akt, and more importantly the phosphorylation state representing activated Akt, increased throughout the hypertrophy process. By 14 days, the total amount of Akt increased fourfold over control, whereas the level of phosphorylated/activated form increased ninefold in the hypertrophying plantaris (Fig. 2a) as determined by densitometry. Akt seems to promote protein synthesis in several ways. For example, Akt phosphorylates glycogen synthase kinase 3β (GSK-3β), leading to its inhibition and the upregulation of protein synthesis[17,18]. More extensively characterized is the ability of Akt to activate p70^{S6K} and PHAS-1/4E-BP1, presumably through mTOR, although this is controversial and has not been proved *in vivo*[7,16,19,20]. Phosphorylation of p70^{S6K} leads to its activation and to the promotion of protein synthetic pathways, whereas phosphorylation of PHAS-1/4E-BP1 releases it from within an inhibitory complex with the translation initiation factor eIF4E, thereby permitting the binding of eIF4E to eIF4G and promoting translation initiation. Consistent with a crucial role for the Akt pathway during muscle hypertrophy *in vivo*, the above Akt-inducible events were noted in hypertrophying plantaris. That is, in addition to Akt phosphorylation, GSK-3β phosphorylation and inhibition were noted (Fig. 2b, c). Furthermore, downstream targets of mTOR were clearly involved, as p70^{S6K} was inducibly phosphorylated and activated (Fig. 2b, d), whereas PHAS-1/4E-BP1 was released from eIF4E (Fig. 2e), allowing its binding to eIF4G (Fig. 2f).

The above findings indicate that the Akt pathway and its downstream targets are activated during muscle hypertrophy *in vivo*. To begin to determine the role of these activations, we used treatment *in vivo* with rapamycin, a quite specific inhibitor of one important Akt target, mTOR. Rapamycin binds to its intracellular receptor,

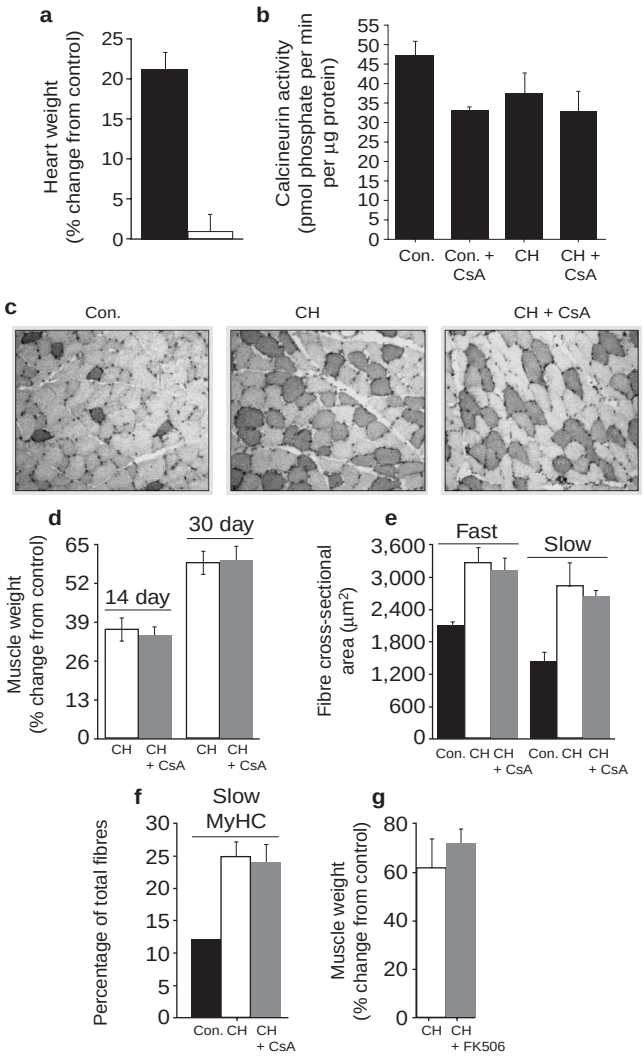

Figure 1 **Muscle hypertrophy is not blocked by CsA. a**, Weight of the rat heart, expressed as percentage change from control, after daily treatment with the β_2-adrenergic agonist clenbuterol (3 mg kg^{-1}, subcutaneously) for 14 d (filled columns) or daily treatment with clenbuterol and cyclosporin for 14 d (open columns) (10 rats per group). **b**, Calcineurin phosphatase activity measured in plantaris muscle lysates from control rats (Con.), control rats treated with cyclosporin for 4 d (Con + CsA), 4-d compensatory hypertrophy rats (CH), and 4-d CH rats treated with cyclosporin (CH + CsA). The total amount of calcineurin was similar between groups as measured by western blotting. **c**, Cross-sections of the rat plantaris muscle stained with an anti-MyHC slow antibody. Groups were control (Con.), 14 d compensatory hypertrophy (CH) and 14 d CH treated daily with cyclosporin (CH + CsA). **d**, Weight of the rat plantaris muscle, expressed as percentage change from control, after 14 or 30 d of compensatory hypertrophy with vehicle (CH) or cyclosporin treatment (CH + CsA) (10 rats per group). **e**, Cross-sectional area of muscle fibres in the rat plantaris muscle of control (Con.), 14 d compensatory hypertrophy (CH) or 14 d compensatory hypertrophy plus cyclosporin treatment (CH + CsA) (five rats per group). Muscle fibres were classified as slow or fast on the basis of immunohistochemical staining with anti-MyHC slow and fast antibodies. **f**, Percentage of muscle fibres expressing slow MyHC in the plantaris muscle of control (Con.), 14 d compensatory hypertrophy (CH) or 14 d compensatory hypertrophy plus cyclosporin treatment (CH + CsA) (five rats per group). **g**, Weight of mouse plantaris muscle, expressed as percentage change from control, after 7 d of compensatory hypertrophy with vehicle (CH) or FK506 treatment (CH + FK506) (10 mice per group).

FKBP12, forming a complex that then binds to and inhibits mTOR activity[7]. Consistent with the biochemical site of rapamycin action was our observation that treatment with rapamycin *in vivo* did not alter the phosphorylation or activity of Akt itself or of its mTOR-independent target GSK-3β (Fig. 2b, c), but instead specifically blocked targets known to be downstream of mTOR[12–17], such as the phosphorylation and activation of $p70^{S6K}$ (Fig. 2b, d) and the release of inhibition of eIF4E by PHAS-1/4E-BP1 (Fig. 2e, f). Most importantly, treatment with rapamycin *in vivo* almost completely prevented the hypertrophic increases in plantaris muscle weight (Fig. 2g) and fibre size (Fig. 2h) at 7 and 14 days. Treatment with rapamycin produced no non-specific effects; that is, there was no effect on body weight or the baseline weight of non-overloaded hindlimb muscles in these animals. Further, rapamycin given to control (surgically untreated) adult animals for 14 days had no effect on body weight or muscle weight (data not shown). In addition to the above results from rats, similar results were obtained when this hypertrophy model was performed in mice (data not shown).

These data demonstrate that during adaptive hypertrophy in adult animals, Akt and its downstream targets, GSK-3β, $p70^{S6K}$ and PHAS-1/4E-BP1, are phosphorylated; moreover, the finding that specific inhibition of mTOR with rapamycin leads to a 95% blockage of hypertrophy indicates that the activation of mTOR and its targets, $p70^{S6K}$ and PHAS-1/4E-BP1, are necessary for adaptive hypertrophy.

To extend the above findings to other models of skeletal muscle hypertrophy, we next focused on the recovery of muscle weight after atrophy through disuse. Although increases in the load on a muscle result in muscle hypertrophy, decreased use of a muscle results in atrophy, as occurs when the hindlimbs of rodents are suspended and no longer work against gravity[21]. Atrophied hindlimb muscles, when reloaded after a period of disuse, undergo a hypertrophic recovery of their original muscle weight over the course of weeks[21]. Depending on the particular hindlimb muscle examined, muscles from rats undergoing hindlimb suspension (HLS) for 14 days showed a 25–55% loss of muscle weight (Fig. 3c, d). After release from HLS, the atrophied muscles were reloaded and hypertrophied, achieving a 15–20% recovery in muscle weight after 7 days of reloading (Fig. 3c, d). As seen in the previous hypertrophy model, the activation of Akt and its targets was correlated with the trophic state of the muscle during both atrophy through disuse and hypertrophy on recovery. That is, Akt protein and phosphorylation levels decreased markedly during the atrophy accompanying HLS (Fig. 3a, second set of lanes), as did the activation state of $p70^{S6K}$ (Fig. 3a, second set of lanes), whereas the PHAS-1/4E-BP1 inhibitory complex with eIF4E increased (Fig. 3b, second column). These changes reverted during recovery of the muscle when it was removed from HLS (Fig. 3a, third set of lanes, and Fig. 3b, third column).

As with the compensatory hypertrophy model described above, not only was activation of the Akt/mTOR pathway correlated with muscle trophic changes in the HLS model, but, more importantly, treatment with the mTOR-inhibitor rapamycin during recovery from suspension markedly blocked the muscle growth observed during the 7-day reloading period (Fig. 3c). Also consistent with the findings in the compensatory hypertrophy model was our observation that CsA had no effect on the recovery of muscle weight during the 7-day reloading period (Fig. 3d).

Taken together, the above findings indicate that the Akt/mTOR pathway is activated in, and requisite for, muscle hypertrophy *in vivo*. To test the hypothesis that activation of mTOR and its downstream targets was not only required for muscle fibre hypertrophy but could actually trigger it, we injected a genetic construct designed to express a constitutively active form of Akt (c.a. Akt)[22] into the tibialis anterior (TA) muscle of adult mice. We have demonstrated that the overexpression of c.a. Akt *in vitro* leads to phosphorylation of $p70^{S6K}$ and PHAS-1/4E-BP1 and to marked

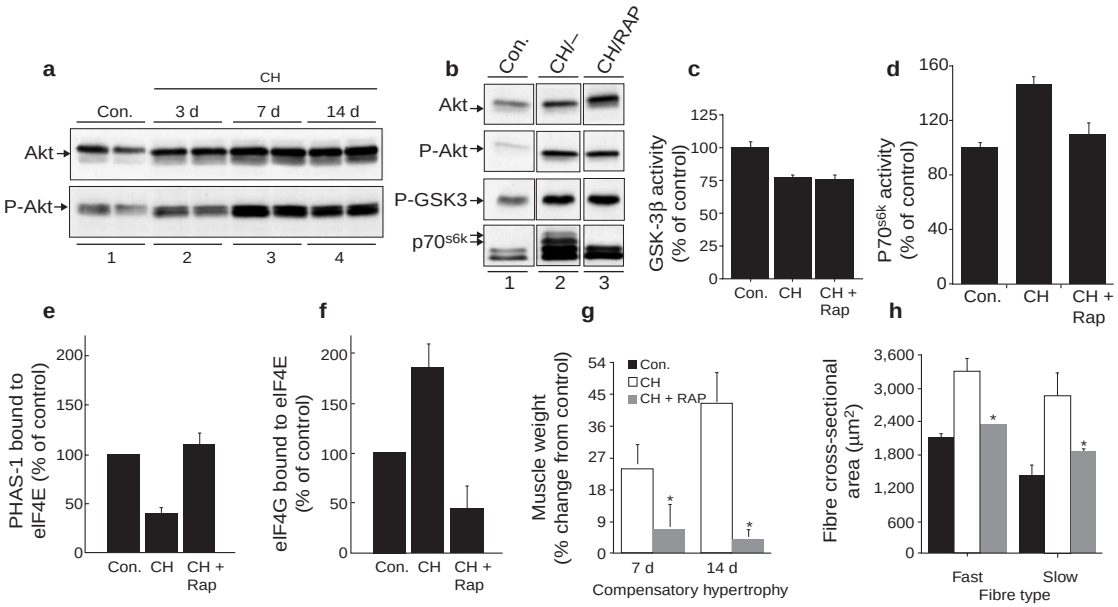

Figure 2 **Muscle hypertrophy is associated with activation of the Akt/mTOR pathway and is blocked by rapamycin. a**, Western blots of native and phosphorylated Akt in the plantaris during compensatory hypertrophy (CH). Each lane represents 200 μg of total protein extracted from a pool of three plantaris muscles after control (Con., lanes 1), 3 d CH (lanes 2), 7 d CH (lanes 3) or 14d CH (lanes 4). For each group, duplicate lanes represent different pools of plantaris muscles. **b**, Western blots of native and phosphorylated Akt, phosphorylated GSK-3β and $p70^{s6k}$ in the rat plantaris. The increase in Akt and GSK-3β phosphorylation measured after 14 d (lane 2) of compensatory hypertrophy (CH/–) was not inhibited by daily injections of rapamycin (CH/Rap; lane 3). The $p70^{s6k}$ gel shift observed after 14 d of compensatory hypertrophy (lane 2) was inhibited by daily injections of rapamycin (CH/Rap; lane 3). Each lane represents 200 μg (Akt and GSK-3β) or 25 μg ($p70^{s6k}$) of total protein extracted from a pool of three plantaris muscles. **c**, The specific activity of GSK-3β was determined by ^{32}P incorporation into phospho-glycogen synthase peptide 2 in the immune complex. The GSK-3β activity was measured in the plantaris of control (Con.); 14 d compensatory hypertrophy (CH) and 14 d CH treated daily with rapamycin (CH + RAP) are shown. **d**, The specific activity of $p70^{s6k}$ was determined by ^{32}P incorporation into 40S ribosomes in the immune complex. The $p70^{s6k}$ activity was measured in the plantaris of control (Con.); 14 d compensatory hypertrophy (CH) and 14 d CH treated daily with rapamycin (CH + Rap) are shown. **e**, PHAS-I/4E-BP1 bound to eIF4E after 14 d compensatory hypertrophy (CH) or 14 d CH treated daily with rapamycin (CH + Rap). After correction for the amounts of eIF4E recovery, the results were expressed as a percentage of the respective controls and are means ± range for two experiments. **f**, eIF4G bound to eIF4E after 14 d compensatory hypertrophy (CH) or 14 d CH plus rapamycin (CH + Rap). After correction for the amounts of eIF4E recovery, the results were expressed as a percentage of the respective controls and are means ± range for two experiments. **g**, Weight of the rat plantaris muscle, expressed as percentage change from control, after 7 or 14 d of compensatory hypertrophy with vehicle (CH) or rapamycin treatment (CH + Rap) (10 rats per group). Asterisk indicates significant difference from CH group ($P < 0.05$). **h**, Cross-sectional area of muscle fibres in the rat plantaris muscle of control (Con.), 14 d compensatory hypertrophy (CH) or 14 d compensatory hypertrophy plus rapamycin treatment (CH + Rap) (five rats per group). Muscle fibres were classified as slow or fast on the basis of immunohistochemical staining with anti-MyHC slow and fast antibodies. Asterisk indicates significant difference from CH group ($P < 0.05$).

hypertrophy of myotubes[6]. The c.a. Akt was fused to enhanced green fluorescent protein (EGFP) and overexpressed under the control of the human skeletal actin promoter[23].

Muscle fibres that had taken up and expressed the activated Akt were identified on the basis of their expression for EGFP (Fig. 4). Those fibres expressing EGFP showed no signs of injury or regeneration. Muscle fibre size was determined in normal TA muscles 7 days after injection with either a plasmid expressing c.a. Akt–EGFP or EGFP alone. In three EGFP-treated and three c.a. Akt-treated normal TA muscles, cross-sectional area was determined in all fibres expressing EGFP (~100 fibres per muscle). Mean fibre size was significantly larger in fibres overexpressing c.a. Akt (2,613 ± 148 μm^2) than in fibres expressing the control EGFP plasmid (1,615 ± 143 μm^2) (Fig. 4a). The distribution of fibre sizes shifted to the right, with the range in fibre sizes increasing from 634–3,873 μm^2 in control muscles to 781–5,347 μm^2 in muscles overexpressing c.a. Akt. Changes in fibre size were evident within 48 h of transfection with c.a. Akt (data not shown). Further, as an additional control, haemagglutinin (HA)-tagged c.a. Akt under the control of the cytomegalovirus (CMV) promoter was tested for its ability to promote fibre growth. Fibres expressing c.a. Akt were identified on the basis of immunohistochemical staining for the HA tag and were found to be larger than control at 2 and 14 days after transfection (data not shown).

Given that overexpression of c.a. Akt could induce hypertrophy of normal fibres, we tested whether c.a. Akt could prevent muscle fibre atrophy. The sciatic nerve was cut, resulting in denervation and atrophy of the TA muscle. Concurrent with the denervation, TA muscles were injected with either the c.a. Akt–EGFP or the EGFP plasmid. At 7 d after the denervation, denervated muscle fibres expressing c.a. Akt were significantly larger than denervated fibres expressing EGFP alone (2,297 ± 73 μm^2 versus 968 ± 17 μm^2) (Fig. 4b). Denervated fibres had a fibre size distribution that was shifted to the left relative to control (410–2,289 μm^2), whereas denervated fibres expressing c.a. Akt had a fibre size distribution that was more similar to control (624–5,716 μm^2). To confirm that c.a. Akt was acting via the mTOR pathway, we showed that the hypertrophy induced by c.a. Akt in normal and denervated fibres could be blocked by the concurrent administration of rapamycin (data not shown). Finally, genetic activation of Akt with a constitutively active PI(3)K construct could also prevent denervation-induced muscle atrophy (data not shown).

Given that genetic activation of Akt could induce hypertrophy and prevent atrophy, we attempted to block endogenous Akt acti-

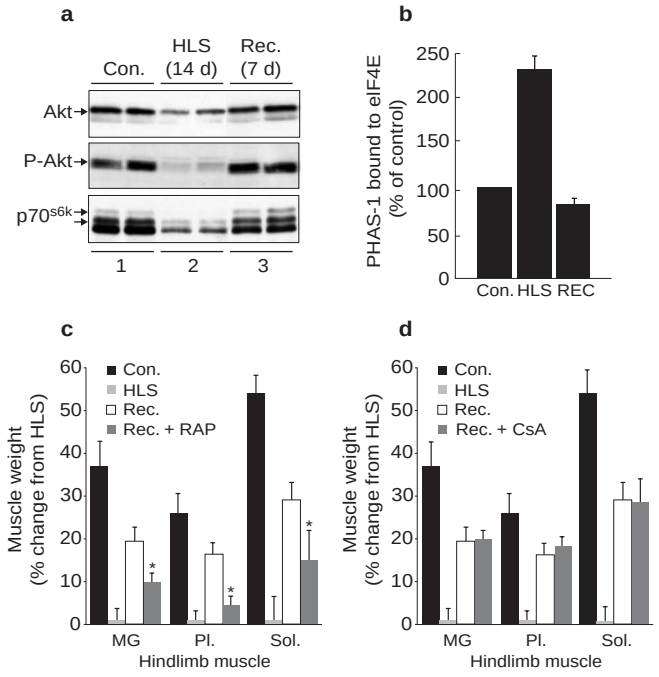

Figure 3 **Recovery of muscle weight after HLS is blocked by rapamycin, but not cyclosporin. a**, Western blots of native and phosphorylated Akt and p70^{s6k} in the medial gastrocnemius (MG) after HLS and recovery (Rec.). Each lane represents 200 μg (Akt) or 25 μg (p70^{s6k}) of total protein extracted from a pool of three MG muscles after control (Con., lanes 1), 14 d HLS (lanes 2) or 14 d HLS followed by 7 d of recovery (lanes 3). For each group, duplicate lanes represent different pools of MG muscles. **b**, PHAS-1/4E-BP1 bound to eIF4E in MG muscle after 14 d of HLS or 14 d of HLS followed by 7 d of recovery (Rec.). After correction for eIF4E recovery, the results were expressed as percentages of the control. Means ± range for two experiments are presented. **c**, Hindlimb muscle weights, expressed as percentage changes from HLS, for the medial gastrocnemius (MG), plantaris (Pl.) and soleus (Sol.) muscles. Muscles were taken after control (con), 14 d of HLS, 14 d of HLS followed by 7 d recovery (Rec.), and 14 d of HLS followed by 7 d of recovery plus treatment with rapamycin (Rec. + RAP) (10 rats per group). Asterisk indicates significant difference between recovery and Rec. + RAP groups ($P < 0.05$). **d**, Hindlimb muscle weights, expressed as percentage changes from 14-d HLS values, for the medial gastrocnemius (MG), plantaris (Pl.) and soleus (Sol.) muscles. Muscles were taken after control (Con.), 14 d of HLS, 14 d of HLS followed by 7 d of recovery (Rec.), and 14 d of HLS followed by 7 d of recovery plus treatment with cyclosporin (Rec. + CsA) (10 rats per group).

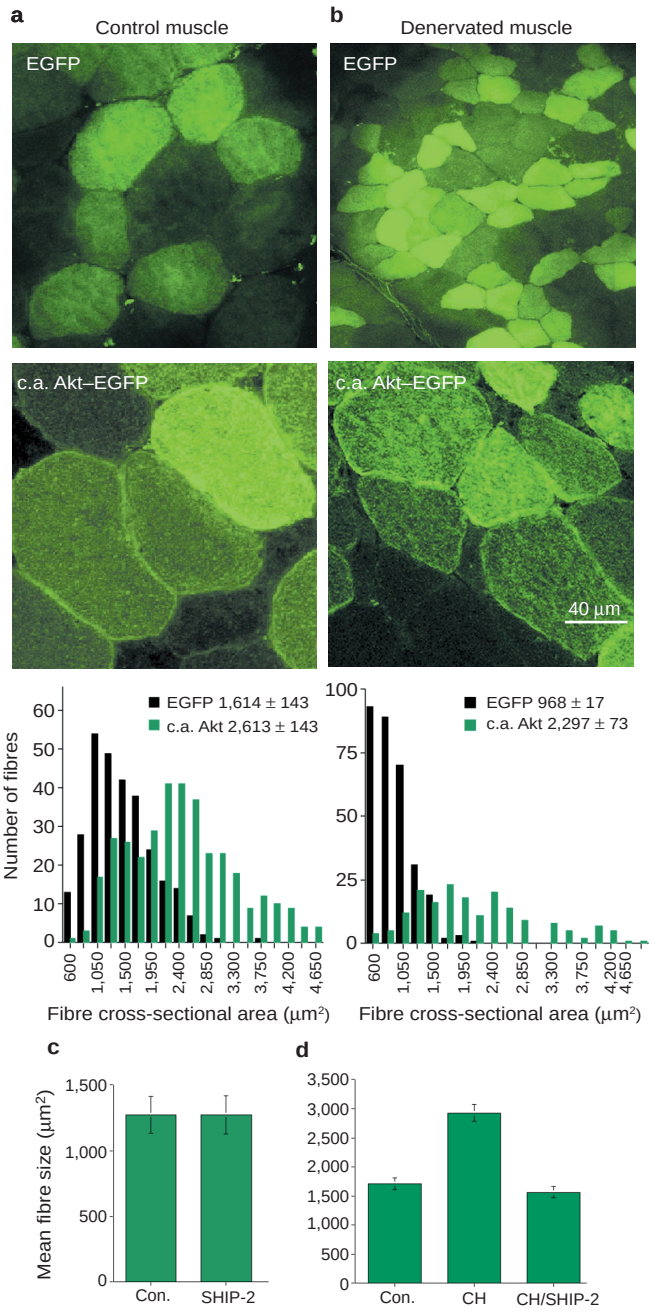

Figure 4 **Expression of activated Akt in normal and denervated muscle fibres induces hypertrophy. a**, **b**, Representative cross-sections of the TA muscle from control and denervated mice. Normal and denervated TA muscles were injected with either a control (EGFP) or an activated Akt (c.a. Akt–EGFP) plasmid. Transfected fibres were identified 7 d after injection and electroporation on the basis of their expression for EGFP. The distribution of cross-sectional areas of EGFP-expressing fibres taken from three muscles under each condition (**a**, control/EGFP, control/c.a. Akt–EGFP; **b**, denervation/EGFP, denervation/c.a. Akt–EGFP) were plotted as frequency histograms. The mean ± s.e.m. is given for each group. **c**, Mean cross-sectional area of muscle fibres in normal mouse TA 7 d after transfection with HSA/EGFP (Con.) or HSA/SHIP-2–HA (SHIP-2). **d**, Mean cross-sectional area of transfected muscle fibres in control and compensatory hypertrophied rat plantaris muscle. The plantaris was surgically overloaded and injected with either HSA/EGFP (CH) or HSA/SHIP-2–HA (CH/SHIP-2) followed by electroporation. Muscle fibre size was determined 7 d after surgery and plasmid injection. Control muscles were analysed 7 d after injection with HSA/EGFP (Con.).

vation genetically by overexpressing the inositol 5-phosphatase SHIP-2, which would independently confirm the above data from the use of rapamycin to block hypertrophy pharmacologically. We have found[6] that the overexpression of SHIP-2 in C2C12 myotubes inhibited IGF-1-induced Akt activation and blocked myotube hypertrophy. Overexpression of SHIP-2 in normal TA muscles had no effect on fibre size (Fig. 4c), which was consistent with the response of rapamycin in normal muscles. In contrast, overexpression of SHIP-2 in fibres of the rat plantaris during compensatory hypertrophy completely blocked the hypertrophy response (Fig. 4d), which was again consistent with the ability of rapamycin to block compensatory hypertrophy pharmacologically.

Skeletal muscles modify their size throughout life in response to changes in external loads and neural activity[1,2]. The signalling pathways responsible for regulating cell size in adult skeletal muscle are poorly understood. Our work demonstrates that adaptive hypertrophy of adult skeletal muscle seems to be crucially regulated by the activation of the Akt/mTOR pathway and its downstream tar-

gets, $p70^{S6K}$ and PHAS-1/4E-BP1. Although our data reveal that maintenance of muscle weight in mature animals is not dependent on the Akt/mTOR pathway (because neither rapamycin nor SHIP-2 produced a loss of muscle weight in adult rodents), this pathway seems to be crucial in load-induced hypertrophy of adult muscle and the recovery of weight after atrophy. Our data go further to show that genetic activation of Akt is sufficient to induce hypertrophy *in vivo* and can oppose the mechanisms responsible for producing muscle atrophy by preserving muscle fibre size.

Contrary to previous reports[24,25], our data suggest that activation of a calcineurin signalling pathway is not crucial for load-induced hypertrophy of skeletal muscle or the switch to expression of slow MyHC. Our conclusions are based on the findings that cyclosporin was unable to block hypertrophy after 7–30 days of daily administration and that calcineurin activity decreased, as opposed to increased, during the hypertrophy process. These conclusions are in disagreement with those of Dunn *et al.*[24], who reported that CsA blocked load-induced hypertrophy when delivered at a dose of 25 mg kg^{-1} twice daily. However, those authors observed a significant decrease in the amount of hypertrophy only at 30 days after the surgical overload, but not at 7 or 14 days while hypertrophy was ongoing and already prominent. Thus, the inability of Dunn *et al.*[24] to block hypertrophy with CsA while it was continuing seems consistent with our conclusion that the calcineurin pathway is not required for the hypertrophy process. Moreover, the late effects of CsA in their hands probably reflect a general toxic effect of long-term, high-dose CsA administration because overall body weight significantly decreased in their long-term-treated animals. The recent findings that tenfold overexpression of activated calcineurin in muscle does not lead to muscle hypertrophy[10] or additional growth after surgical overload[25], and that treatment with cyclosporin does not prevent IGF-1-mediated hypertrophy[26] further supports the conclusion that calcineurin is not involved in a crucial signalling pathway that is necessary for adaptive hypertrophy of muscle fibres in adult rodents.

Our findings are consistent with previous suggestions that overload-induced hypertrophy is due to increases in translational capacity and/or translational efficiency[1,2] because these are processes that indeed seem to be regulated by $p70^{S6K}$ and PHAS-1/4E-BP1 (refs 14, 17, 20). It has been postulated that increases in protein synthesis during compensatory hypertrophy are initially derived through increases in translational efficiency followed later by changes in translational capacity through the addition of myonuclei. Indeed, increases have been found in the number of myonuclei per fibre after compensatory overload[27], and irradiation studies have suggested that satellite-cell incorporation is crucial for compensatory hypertrophy of the rat EDL muscle[28]. However, muscle hypertrophy can occur in the absence of satellite cell proliferation/fusion into myofibres [1,2,29–31]. The mechanisms regulating muscle fibre size are obviously complex, and the degree to which changes in translation efficiency and/or satellite cell proliferation contribute to hypertrophy require further study.

The findings that $p70^{S6K}$ and PHAS-1/4E-BP1 are activated during hypertrophy and that their activation is blocked by rapamycin suggest that mTOR is a crucial regulator of muscle fibre size in adult animals. This regulation of mTOR *in vivo* is likely to be mediated via Akt/protein kinase B (refs 7, 19, 20), which we demonstrated was activated during skeletal muscle hypertrophy and was sufficient to induce the hypertrophy process when introduced genetically. Recent genetic manipulation in *Drosophila* of PI(3)K, Akt and $p70^{S6K}$ have indicated a role of the PI(3)K/Akt/mTOR pathway in the regulation of cell size, in that inactivation of this pathway leads to smaller cells but not fewer cells[32,33]. The role of $p70^{S6K}$ during postnatal growth has also been investigated in mice. Mice with a homozygous disruption of the $p70^{S6K}$/$p85^{S6K}$ gene have lower body weights and organ weights relative to wild-type littermates[34]. Additional support for the role of PI(3)K in muscle growth is provided by a recent study by Shoi *et al.*[35], who demonstrated that cardiac-specific overexpression of a constitutively active PI(3)K in mice led to hearts that were larger than normal, primarily because of an increase in the size of the cardiomyocytes. Interestingly, Murgia *et al.*[11] found that expression of an activated Ras that stimulates PI(3)K led to enhanced regeneration of injured muscle fibres. Further, Baar and Esser[31] demonstrated that phosphorylation of $p70^{S6K}$ increases during high-resistance exercise training and muscle hypertrophy in rats. Lastly, our findings *in vivo* demonstrate that overexpression of activated Akt leads to an increase in muscle fibre size. Activated Akt was capable not only of increasing the size of fibres in normal muscles but also of preserving muscle fibre size in muscles undergoing atrophy. Taken together, these data suggest that activation of mTOR via PI(3)K/Akt might serve as a crucial regulator of muscle fibre growth *in vivo*. By identifying a crucial pathway responsible for regulating skeletal muscle hypertrophy, our work provides an important step in the development of therapeutics for treating muscle atrophy. □

Methods

Procedures *in vivo*.

Female Sprague–Dawley rats (250–275 g) were anaesthetized with ketamine/xylazine (50/10 mg kg^{-1}, intraperitoneally); with the use of aseptic surgical techniques the soleus, medial gastrocnemius and lateral gastrocnemius muscles were removed bilaterally, producing a functional overload on the plantaris muscles[8,9]. In some instances, plasmid DNA (100 µl) was injected into the muscle immediately after the procedure. The hindlimbs of adult female SD rats (225–250 g) were unloaded by suspending their tails with a tail-traction bandage as described[29]. At the appropriate times, rats were killed and hindlimb muscles were removed, weighed and frozen in isopentane cooled with liquid nitrogen. Weight-matched surgically untreated rats served as controls.

The TA muscle was isolated in adult C57BL/6 mice under isoflurane (2–2.5%) anaesthesia. In some mice the right sciatic nerve was isolated in the mid-thigh region and cut, leading to denervation of the lower limb muscles. Plasmid DNA (100 µg) was injected (30 µl) into the muscle along the length of the fibres with the use of a Hamilton syringe. Immediately after the plasmid injection, electric pulses were applied by two stainless steel pin electrodes placed on each side of the isolated muscle belly. Square-wave electric pulses (16 pulses with a duration of 20 ms at a frequency of 1 Hz) were delivered by an ECM 830 electroporation unit (BTX, San Diego, California) at a field strength of 125 V cm^{-1}. All procedures were done in accordance with guidelines set by the Institutional Animal Care and Use Committee.

Drug administration *in vivo*.

Animals were randomized to treatment or vehicle groups so that the mean starting body weights of each group were equal. Drug treatment began on the day of surgery or on the first day of reloading after the 14-day suspension. Rapamycin was delivered once daily by intraperitoneal injection at a dose of 1.5 mg kg^{-1}, dissolved in 2% carboxymethylcellulose. CsA was delivered once daily by subcutaneous injection at a dose of 15 mg kg^{-1}, dissolved in 10% methanol and olive oil. FK506 was delivered once daily via subcutaneous injection at a dose of 3 mg kg^{-1}, dissolved in 10% ethanol, 10% cremophor and saline.

Transfection *in vivo*.

Constructs used encoded the following: (1) myristoylated, c.a. Akt (refs 22, 36) fused in frame at the 3′ end to the gene encoding EGFP (Clontech), and subcloned into an expression vector containing the human skeletal actin (HSA) promoter[23]; or (2) the gene encoding EGFP alone, subcloned into the same expression vector containing the HSA promoter. The c.a. Akt–EGFP fusion protein was tested in C2C12 myotubes, and mediated the activation of $p70^{s6k}$ and PHAS-1/4E-BP1 (data not shown), as expected for c.a. Akt. As an additional control, the myristoylated, HA-tagged c.a. Akt was subcloned into a vector consisting of the CMV promoter. Human inositol 5-phosphatase SHIP-2 was cloned from an Origene library. SHIP-2 was HA-tagged and subcloned into an expression vector containing the human skeletal actin promoter.

Calcineurin phosphatase assay.

Plantaris muscles were homogenized on ice for 15 s in 10 ml of buffer containing 20 mM Tris-HCl pH 7.6, 50 mM NaCl, 1 mM EDTA, 1 mM phenyl methylsulphonyl fluoride (PMSF), 10 µg ml^{-1} leupeptin, 10 µg ml^{-1} aprotinin and 0.1% Nonidet P40. Lysates were cleared by centrifugation at 11,000*g* for 15 min at 4 °C. The supernatant fractions were then desalted in G-25 Sephadex columns (Boehringer Mannheim) equilibrated in lysis buffer. The total phosphatase activity (serine/threonine phosphatase assay system; Promega) in the lysates was determined in the presence of calmodulin (250 µg ml^{-1}) and calculated from the difference in absorbance read in the presence and absence of both phosphopeptide substrate and okadaic acid. Phosphate release was measured at 30 °C for 2 min.

Western blots.

Muscles were homogenized at 4 °C in RIPA lysis buffer (1% Nonidet P40, 0.5% sodium deoxycholate, 0.1% SDS in 50 mM NaCl, 20 mM Tris-HCl pH 7.6) containing 1 mM PMSF, 10 µg ml^{-1} aprotinin, 10 µg ml^{-1} leupeptin, 5 mM benzamidine, 1 mM EDTA, 5 mM *N*-ethylmaleimide, 50 mM NaF, 25 mM β-glycerophosphate, 1 mM sodium orthovanadate, 100 nM okadaic acid and 5 nM microcystin LR. Homogenates were clarified by centrifugation at 12,000*g* for 20 min before determination of protein

concentration by bicinchoninic acid assay (Pierce Chemical Co.). SDS–PAGE was performed on 7.5% gels prepared with an acrylamide:bisacrylamide ratio of 100:1. Western blots were revealed with enhanced chemiluminescence (Renaissance; NEN). Antibodies against anti-p70^{s6k} (C-18; Santa Cruz) and Akt (NEB) were used to detect protein expression levels. Antibodies against Akt phosphorylated on Ser 473 (NEB) and GSK-3α/β phosphorylated on Ser 21/9 (NEB) were used to detect the catalytically activated form of the kinase.

Kinase assay of p70^{s6k}.

Protein A–agarose beads (Bio-Rad; 0.1 ml of serum per ml of packed beads) were incubated at 23 °C for 60 min with nonimmune serum or antisera against p70^{s6k}. The beads were then washed five times with PBS (145 nM NaCl, 4 mM KCl, 10 mM sodium phosphate pH 7.4) and once with homogenization buffer. Samples of extract (100 µl) were incubated with beads (10 µl) for 60 min at 4 °C with constant mixing and then washed twice (0.5 ml of homogenization buffer per wash) and suspended in 100 µl of homogenization buffer. To measure p70^{s6k} activity, immune complexes were incubated with 10 µl of solution containing 50 mM sodium β-glycerophosphate (pH 7.4), 14 mM NaF, 10 mM $MgCl_2$, 1 mM dithiothreitol, 9 µM cAMP-dependent protein kinase inhibitory peptide, 20 µM calmidazolium, 200 µM [γ-^{32}P]ATP (300–500 c.p.m./pmol) and 40S ribosomes (2 mg ml^{-1} final concentration)[37].

Quantification of PHAS-1–eIF4E and eIF4E–eIF4G complexes.

Each frozen muscle was placed in a liquid-nitrogen-chilled porcelain mortar to which 0.5 ml of the following homogenization buffer (pH 7.0) was added: 50 mM NaF, 50 mM β-glycerophosphate, 0.1 mM microcystin-LR, 10 mM potassium phosphate, 10 mM $MgCl_2$, 1 mM EDTA, 1 mM EGTA, 1 mM sodium vanadate, 0.1% Tween 20, 1 mM PMSF, 1 mM benzamidine, 10 µg ml^{-1} leupeptin and 10 µg ml^{-1} aprotinin. The tissue was ground into powder, which was placed in a glass homogenization tube and left to thaw while being homogenized with a Teflon pestle driven at 1,000 r.p.m. The homogenates were centrifuged at 10,000*g* for 30 min and the protein concentration of the supernatant fractions was determined. eIF4E-bound forms of PHAS-1/4E-BP1 and eIF4G were isolated by affinity-purification of the complexes with m^{7}GTP-Sepharose (Pharmacia)[16]. In brief, samples (1 mg protein/500 µl) of extract were incubated with resin (30 µl) packed beads for 30 min at 4 °C. The beads were then washed three times (1 ml buffer per wash) before proteins were eluted with SDS-sample buffer. PHAS-1/4E-BP1 and eIF4E were detected with the antibodies and immunoblotting procedures described previously[16]. eIF4G was detected by immunoblotting with an antibody generated against a peptide (CQKEFEKDKDDDEVFEKKQKEMDEA; single-letter amino acid abbreviations) corresponding to a sequence in eIF4G. In brief, the rabbits were immunized with peptide (0.5 mg peptide per injection) that had been conjugated to keyhole limpet haemocyanin, and boosted with the conjugate at monthly intervals. Antibodies were affinity-purified with a resin prepared by coupling the peptide via its amino-terminal cysteine to SulfoLink (Pierce). After the column had been washed, antibodies were eluted at pH 2.7, neutralized immediately and isolated after a final purification step with Protein A–agarose.

Data analysis.

Muscle fibre size was obtained from digitally imaged serial cross-sections of cryostat-sectioned muscle. Individual muscle fibres were outlined and cross-sectional area was determined with a computer-assisted image analysis system (MetaMorph™; Universal Imaging Corporation). All data are expressed as means ± s.e.m. (represented as error bars). A one-way analysis of variance with Fisher's post-hoc correction for multiple paired comparisons was used for comparisons between groups. Statistical significance was set at $P < 0.05$.

RECEIVED 9 APRIL 2001; REVISED 18 JULY 2001; ACCEPTED 18 JULY 2001;
PUBLISHED 10 OCTOBER 2001.

1. Carson, J. A. *Exercise Sport Science Rev.* **25,** 301–320 (1997).
2. Baar, K., Blough, E., Dineen, B. & Esser, K. *Exercise Sport Science Rev.* **27,** 333–379 (1999).
3. Molkentin, J. D. *et al. Cell* **93,** 215–228 (1998).
4. Semarian, C. *et al. Nature* **400,** 576–581 (1999).
5. Musaro, A. *et al. Nature* **400,** 581–585 (1999).
6. Rommel, C. *et al. Nature Cell Biol.* **3,** 1009–1013 (2001).
7. Schmeizie, T. & Hall, M. N. *Cell* **103,** 253–262 (2000).
8. Adams, G. R. & Haddad, G. R. *J. Appl. Physiol.* **81,** 2509–2516 (1996).
9. Roy, R. R. *et al. J. Appl. Physiol.* **83,** 280–290 (1997).
10. Naya, F. J. *et al. J. Biol. Chem.* **275,** 4545–4548 (2000).
11. Murgia, M. *et al. Nature Cell Biol.* **2,** 142–147 (2000).
12. Terada, N. *et al. Proc. Natl Acad. Sci. USA* **91,** 11477–11481 (1994).
13. Brunn, G. J. *et al. Science* **277,** 99–101 (1997).
14. Rhoads, R. E. *J. Biol. Chem.* **274,** 30337–30340 (1999).
15. Lin, T.-A. *et al. Science* **266,** 653–656 (1994).
16. Lin, T.-A. & Lawrence, J. C. Jr *J. Biol. Chem.* **271,** 30199–30204 (1996).
17. Jefferson, L. S., Fabian, J. R. & Kimball, S. R. *Int. J. Biochem. Cell Biol.* **31,** 191–200, (1999).
18. Welch, G. I., *et al. FEBS Lett.* **410,** 418–422 (1997).
19. Tung, C. O., Rittenhouse, S. E. & Tsichlis, P. N. *Annu. Rev. Biochem.* **68,** 965–1014 (1999).
20. Shah, O.J, Anthony, J. C., Kimball, S. R. & Jefferson, L. S. *Am. J. Physiol. Endocrinol. Metab.* **279,** E715–E729 (2000).
21. Thomason, D. B., Herrick, R. E., Surdyka, D. & Baldwin, K. M. *J. Appl. Physiol.* **63,** 130–137 (1987).
22. Eves, E. M. *et al. Mol. Cell. Biol.* **18,** 2143–2152 (1998).
23. Brennan, K. J. & Hardeman, E. C. *J. Biol. Chem.* **268,** 719–725 (1993).
24. Dunn, S. E., Burns, J. L. & Michel, R. N. *J. Biol. Chem.* **274,** 21908–21912 (1999).
25. Dunn, S. E., Chin, E. R. & Michel, R. N. *J. Cell Biol.* **151,** 663–672 (2000).
26. Musaro, A. *et al. Nature Genet.* **27,** 195–200 (2001).
27. Roy, R. R., Monke, S. R., Allen, D. L. & Edgerton, V. R. *J. Appl. Physiol.* **87,** 634–642 (1999).
28. Rosenblatt, J. D., Yong, D. & Parry, D. J. *Muscle Nerve* **17,** 608–613 (1994).
29. Wong, T. S. & Booth F. W. *J. Appl. Physiol.* **69,** 1718–1724 (1990).
30. Lowe, D. A. & Always, S. E. *Cell Tiss. Res.* **296,** 531–539 (1999).
31. Baar, K. & Esser, K. *Am. J. Physiol. Cell* **45,** C120–C127 (1999).
32. Montagne, J. *et al. Science* **285,** 2126–2129 (1999).
33. Weinkove, D. & Leever, S. J. *Curr. Opin. Genet. Dev.* **10,** 75–80 (2000).
34. Shima, H. *et al. EMBO J.* **17,** 6649–6659 (1998).
35. Shioi, T. *et al. EMBO J.* **19,** 2537–2548 (2000).
36. Rommel, C. *et al. Science* **286,** 1738–1741 (1999).
37. Azpiazu, I, Saltiel, A. R., DePaoli-Roach, A. A. & Lawrence, J. C. Jr *J. Biol. Chem.* **271,** 5033–5039 (1996).

ACKNOWLEDGEMENTS

We thank L. S. Schleifer and P. R. Vagelos and the rest of the Regeneron community for their support, particularly E. Burrows for graphics work and C. Rommel for insightful discussions.
Correspondence and requests for materials should be addressed to S.C.B. or G.D.Y.